



28 25



METRIC BY RESOLUTION TEST CHART
NBS 1963-A

AD A11 3138

12

AFGL-TR-82-0003
ENVIRONMENTAL RESEARCH PAPERS, NO. 760



Composition and Structure Measurements in an Ionospheric Barium Cloud

R. NARCISI
E. TRZCINSKI
G. FEDERICO
L. WLODYKA
P. BENCH

23 December 1981

Approved for public release; distribution unlimited.

This work was supported in part by the Defense Nuclear Agency under Subtask I25AAXHX,
Work Unit 00014 entitled "Nuclear Weapons Effects Program."

AERONOMY DIVISION PROJECT 2310
AIR FORCE GEOPHYSICS LABORATORY
HANSCOM APB, MASSACHUSETTS 01731

DTIC
ELECTE
S APR 7 1982
A

AIR FORCE SYSTEMS COMMAND, USAF



82 04 07 042

DTIC FILE COPY

This report has been reviewed by the ESD Public Affairs Office (PA)
and is releasable to the National Technical Information Service (NTIS).

This technical report has been reviewed and
is approved for publication.

Alva T. Stair, Jr.

DR. ALVA T. STAIR, Jr
Chief Scientist

Qualified requestors may obtain additional copies from the
Defense Technical Information Center. All others should apply
to the National Technical Information Service.

Unclassified

SECURITY CLASSIFICATION OF THIS PAGE (When Data Entered)

REPORT DOCUMENTATION PAGE		READ INSTRUCTIONS BEFORE COMPLETING FORM
1. REPORT NUMBER AFGL-TR-82-0003	2. GOVT ACCESSION NO. AD-A112 138	3. RECIPIENT'S CATALOG NUMBER
4. TITLE (and Subtitle) COMPOSITION AND STRUCTURE MEASUREMENTS IN AN IONOSPHERIC BARIUM CLOUD	5. TYPE OF REPORT & PERIOD COVERED Scientific. Final.	
	6. PERFORMING ORG. REPORT NUMBER ERP No. 760	
7. AUTHOR(s) R. Narcisi L. Wlodyka E. Trzcinski P. Bench G. Federico	8. CONTRACT OR GRANT NUMBER(s)	
9. PERFORMING ORGANIZATION NAME AND ADDRESS Air Force Geophysics Laboratory (LKD) Hanscom AFB Massachusetts 01731	10. PROGRAM ELEMENT PROJECT, TASK AREA & WORK UNIT NUMBERS 61102F 2310G310	
11. CONTROLLING OFFICE NAME AND ADDRESS Air Force Geophysics Laboratory (LKD) Hanscom AFB Massachusetts 01731	12. REPORT DATE 23 December 1981	
	13. NUMBER OF PAGES 31	
14. MONITORING AGENCY NAME & ADDRESS (if different from Controlling Office)	15. SECURITY CLASS. (of this report) Unclassified	
	15a. DECLASSIFICATION DOWNGRADING SCHEDULE	
16. DISTRIBUTION STATEMENT (of this Report) Approved for public release; distribution unlimited.		
17. DISTRIBUTION STATEMENT (of the abstract entered in Block 20, if different from Report)		
18. SUPPLEMENTARY NOTES This work was supported in part by the Defense Nuclear Agency under Subtask I25AAXHX, Work Unit 00014 entitled "Nuclear Weapons Effects Program."		
19. KEY WORDS (Continue on reverse side if necessary and identify by block number) Barium ion cloud Ionospheric irregularities Rocket measurements Barium striations Ion composition Image cloud Plasma chemistry Outgassing water vapor		
20. ABSTRACT (Continue on reverse side if necessary and identify by block number) A 48 kg barium payload was launched from Eglin Air Force Base, Florida on 12 December 1980 at 2311 GMT and detonated at 133.7 km. At 2342:50.25 GMT, a second rocket, instrumented with an ion mass spectrometer and pulsed plasma probes, was fired to traverse the barium cloud. Composition, ion density, and structure measurements were acquired up to 241.2 km in both the natural and disturbed ionosphere. The rocket penetrated the barium cloud between 147 and 184 km. In addition to the Ba ⁺ , Ba ⁺⁺ produced by H Lyman α ionization, and Ca ⁺ , an impurity in the barium, were		

DD FORM 1 JAN 73 1473

Unclassified

SECURITY CLASSIFICATION OF THIS PAGE (When Data Entered)

Unclassified

SECURITY CLASSIFICATION OF THIS PAGE(When Data Entered)

20. (Cont)

detected in the cloud. A peak barium ion concentration of about 6×10^6 ions cm^{-3} was measured at 161 km where the ionospheric NO^+ and O_2^+ ions were essentially eliminated by large recombinative loss. The bottom side of the barium cloud had a relatively smooth structure while the top side showed significant density fluctuations. The first experimental evidence of a theoretically predicted E region "image cloud" was found in the form of an enhanced NO^+ layer just below the barium cloud. Unexplained wave-like density variations in O^+ , NO^+ , and O_2^+ also were seen above the barium cloud to 195 km. A quantitative estimate of the outgassing water vapor concentrations near the payload's surface was made using the fast charge transfer rate coefficient for $\text{O}^+ + \text{H}_2\text{O} \rightarrow \text{H}_2\text{O}^+ + \text{O}$ that created the observed water vapor ions. It was determined that the measured H_2O^+ ions were produced within 3 to 4 cm of the sampling plate's surface and that the average H_2O pressure over this distance was constant on ascent at 8×10^{-6} Torr within a factor of two.

Unclassified

SECURITY CLASSIFICATION OF THIS PAGE(When Data Entered)

Preface

Funding for the ion mass spectrometer measurements was provided mostly by the Air Force Office of Scientific Research under Task 2310G3. The Defense Nuclear Agency supplied the rocket integration and launch costs. We thank Dr. E. P. Szuszcwicz for his advocacy and cooperation in conducting this experiment. Finally, we acknowledge the Sandia National Laboratories for their excellent rocket and payload integration support.



A

Contents

1. INTRODUCTION	7
2. INSTRUMENTATION AND MEASUREMENT PROGRAM	8
3. RESULTS AND DISCUSSION	10
4. CONCLUSION	21
REFERENCES	23
DISTRIBUTION LIST	24

Illustrations

1. Payload Instrumentation and Flight Events	9
2. Schematic of the Quadrupole Ion Mass Spectrometer	10
3. Spectrometer Program for the Measurement of Selected Ion Mass Numbers at High Spatial Resolution	11
4. Ascent Measurements Showing the Penetration of the Barium Cloud and its Effects on the Normal Ambient Species NO^+ , O_2^+ and O^+	12
5. Distributions of Constituents From the Barium Release	14
6. The NO^+ Profile Measured on Ascent	15
7. The O_2^+ Profile Measured on Ascent	16
8. Ascent Measurements of O^+ and the Contaminant H_2O^+	17

Illustrations

- | | | |
|-----|---|----|
| 9. | A Comparison of the Ascent and Descent Aperture Plate Current Measurements Showing the Smooth Ionosphere Adjacent to the Barium Cloud | 19 |
| 10. | An Expanded Plot of the Ascent and Descent Aperture Plate Current Measurements in the Vicinity of the Barium Cloud | 20 |

Tables

- | | | |
|----|---|---|
| 1. | Event JAN Probe Payload Trajectory Tabulation Excerpted From a Single Station Radar Solution Prior to Smoothing | 8 |
|----|---|---|

Composition and Structure Measurements in an Ionospheric Barium Cloud

1. INTRODUCTION

The only *in situ* measurements of atmospheric barium releases are those of the electron density structure performed by Baker and Ulwick¹ as part of the Defense Nuclear Agency's (DNA) STRESS program. Kelley et al² analyzed the STRESS results and demonstrated that the late-time barium striations agree with non-linear Rayleigh-Taylor instability development; the same mechanism believed to create equatorial Spread F.

This report describes the first measurements of the ion composition and structure made in a barium cloud. The effort was part of the DNA PLACES (Position Location and Communication Effects Simulations) program. The barium/probe rocket pair and associated measurements were further designated as event "JAN." The barium payload was launched from the Eglin Air Force Base, Florida, Test Range on 12 December 1980 at 2311 GMT releasing 48 kg of barium at 183.7 km. At 2342:50.25 GMT a Terrier Tomahawk rocket payload was launched containing an

(Received for publication 21 December 1981)

1. Baker, K. D., and Ulwick, J. C. (1978) Measurements of electron density structure in striated barium clouds, Geophys. Res. Lett. 5:723.
2. Kelley, M. C., Baker, K. D., and Ulwick, J. C. (1979) Late time barium cloud striations and their possible relationship to equatorial Spread-F, J. Geophys. Res. 84:1898.

ion mass spectrometer and pulsed plasma probes targeted to penetrate the barium cloud. In this report we present the instrumentation, measurement technique, the data, and some implications of the measurements from the ion mass spectrometer.

2. INSTRUMENTATION AND MEASUREMENT PROGRAM

The mass spectrometer was mounted at the forward end of the payload along the vehicle's axis. Figure 1 shows the payload configuration and flight functions. Trajectory parameters are given in Table 1. The spectrometer was activated following nose cone release that simultaneously removed the instrument's vacuum cap. The payload included an attitude control system (ACS) that aligned the payload's axis with the magnetic field to minimize perturbations on the pulsed plasma probes. The ACS maintained the payload to within $\pm 5^\circ$ of the magnetic field on ascent and most of descent. Also, the roll rate was held to less than $\pm 0.6^\circ \text{ sec}^{-1}$. Nevertheless, the angle of attack between the velocity vector and the spectrometer axis was still favorable since the rocket was launched essentially along the magnetic field. The attack angle was less than 25° to about 200 km on upleg, increased above this altitude, and became large on descent.

Table 1. Event JAN Probe Payload Trajectory Tabulation Excerpted From a Single Station Radar Solution Prior to Smoothing

Time After Lift-Off (sec)	GMT	Altitude (km)	Range (km)	Latitude	Longitude	Velocity km/sec
50.55	2343:40.8	68.83	76.64	30.0855	86.8274	2.05
100.55	2344:30.8	146.05	167.31	29.6615	86.8717	1.65
150.55	2345:20.8	200.63	238.71	29.2428	86.9211	1.29
200.55	2346:10.8	232.11	291.46	28.8321	86.9735	1.04
245.8	2346:56.1	241.22	325.28	28.464	87.0227	0.94
250.55	2347:0.8	241.13	328.09	28.4265	87.0277	0.94
300.55	2347:50.8	227.91	352.19	28.0193	87.0830	1.05
350.55	2348:40.8	198.22	368.53	27.6732	87.3808	1.31
400.55	2349:30.8	133.24	384.03	27.1886	87.1935	1.68
448.55	2350:18.8	54.29	407.36	26.7800	87.2469	2.31

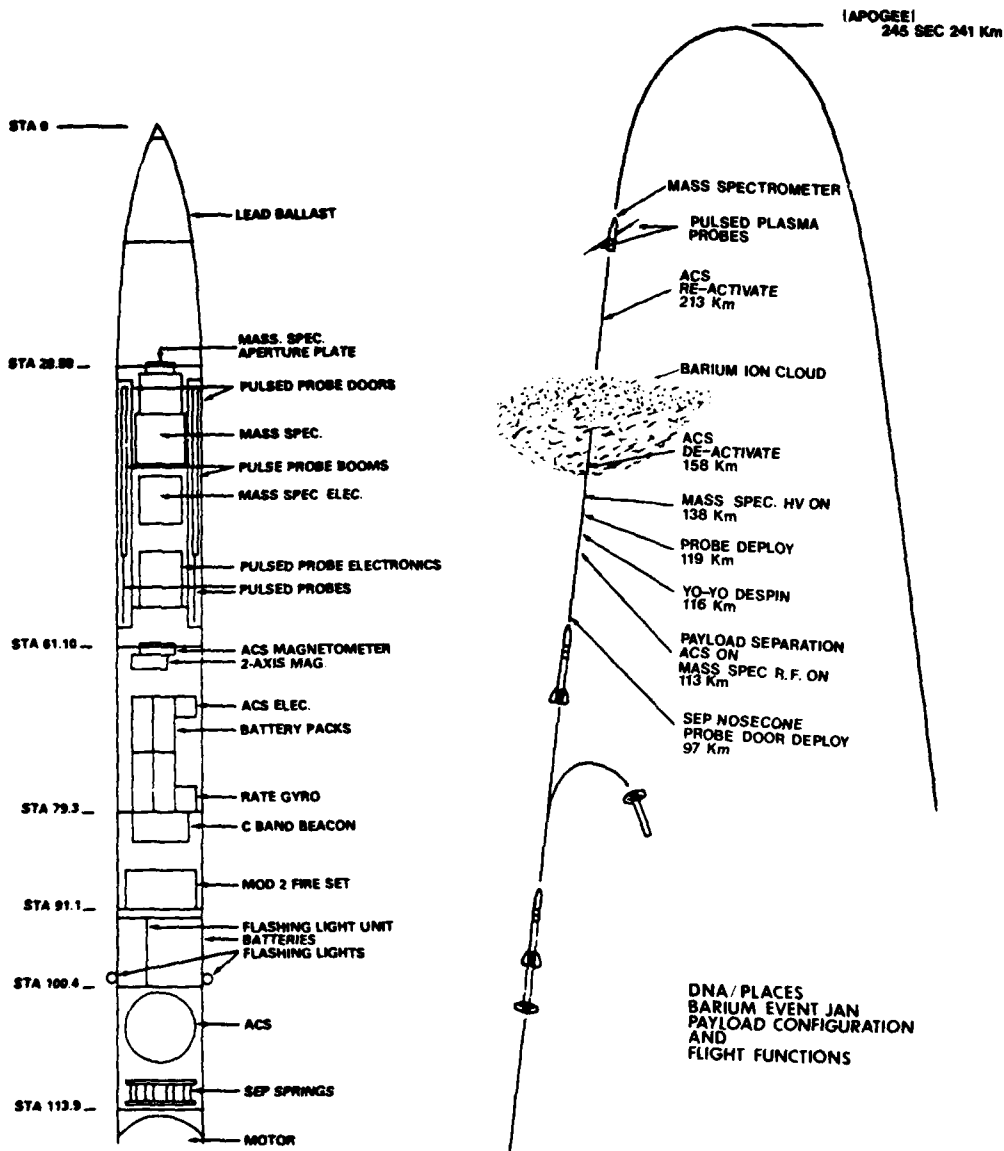


Figure 1. Payload Instrumentation and Flight Events

Figure 2 shows a schematic of the quadrupole ion mass spectrometer. The two significant data outputs were the total positive ion current collected on the aperture

plate for ionospheric structure measurements and the mass spectra output for species composition. The spectrometer measurement program is presented in Figure 3. Sixty-four masses were sampled digitally for 10 msec each, yielding a total program period of 0.64 sec. Mass number repetitions provided measurements with high spatial resolution. Above 145 km, the aperture plate output had a 1 to 1.5 m altitude resolution (varying with vehicle velocity) while the barium and oxygen ion measurements had a resolution of 50 to 65 m. The species identifications for the associated mass numbers in Figure 3 are $14(\text{N}^+)$, $16(\text{O}^+)$, [contaminants from outgassing water vapor: $17(\text{OH}^+)$, $18(\text{H}_2\text{O}^+)$, and $19(\text{H}_3\text{O}^+)$], $23(\text{Na}^+)$, $24(\text{Mg}^+)$, $27(\text{Al}^+)$, $28(\text{Si}^+)$, $30(\text{NO}^+)$, $32(\text{O}_2^+)$, $40(\text{Ca}^+)$, $56(\text{Fe}^+)$, $69(\text{Ba}^{++})$, $136-138(\text{Ba}^+)$. The remaining mass numbers were selected to establish background levels. The barium isotopes of 136 and 138 amu with relative abundances of 7.81% and 71.66%, respectively, were chosen to provide an added factor of about 9 in sensitivity in case 138 went off scale (exceeding 10^7 ions cm^{-3}).

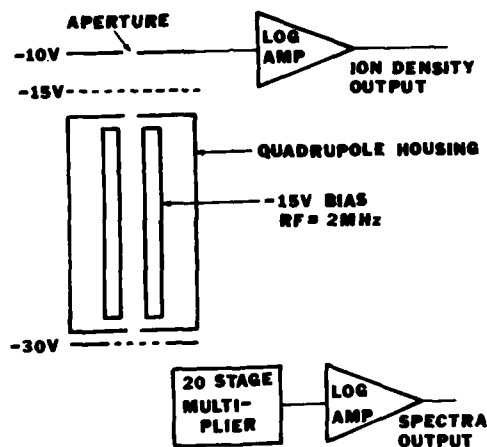


Figure 2. Schematic of the Quadrupole Ion Mass Spectrometer

3. RESULTS AND DISCUSSION

Composition measurements were acquired between 142 and 241.2 km on upleg and on downleg to 180 km, below which the large angle of attack caused signal drop-out. The ion species measured, included O^+ , NO^+ , O_2^+ , Ba^+ , Ba^{++} , Ca^+ , and H_2O^+ ; all other species were below the set detection limit of about 40 ions cm^{-3} .

MASS PROGRAM					
SEQUENCE #	MASS # - AMU				
1.	16	14	30	136	138
2.	16	14	32	136	138
3.	16	14	30	136	138
4.	16	14	32	136	138
5.	16	14	30	136	138
6.	16	14	32	136	138
7.	16	14	30	136	138
8.	16	14	32	136	138
9.	16	14	30	136	138
10.	13	14	15	16	17
11.	18	19	21	23	24
12.	27	28	30	32	69
13.	136	138	40	56	

SAMPLE RATE: 10 MS/AMU
PROGRAM TIME: 0.64 SECONDS

Figure 3. Spectrometer Program for the Measurement of Selected Ion Mass Numbers at High Spatial Resolution

The results are presented in terms of the measured species currents vs altitude. To obtain absolute density values to within $\pm 50\%$ for all species below about 225 km, the following conversion factors may be applied: for NO^+ , O_2^+ , and H_2O^+ , 1×10^{12} ions cm^{-3} amp $^{-1}$; for O^+ , 8×10^{11} ions cm^{-3} amp $^{-1}$; and for Ba^+ , Ca^+ , and Ba^{++} , 1.3×10^{12} ions cm^{-3} amp $^{-1}$. The accuracy in the species densities can be improved somewhat by normalizing to the more precise electron concentrations from the pulsed plasma probes.³

Figure 4 shows the ascent measurements of O^+ , NO^+ , O_2^+ , and Ba^+ . It is seen that the barium cloud was entered at 147 km and exited at 184 km. The peak barium ion concentration (including all isotopes) was about 6×10^6 ions cm^{-3} near 161 km. The underside structure of the barium cloud was relatively smooth; the small bite-out at 158 km was due to a nitrogen gas burst from the ACS nozzle. (The ACS was deactivated slightly above this altitude and reactivated at 213 km on upleg but no nozzle fire occurred until 178 km on descent.) In contrast, the topside of the barium cloud had significant density fluctuations. The NO^+ and O_2^+ ions were, as expected,

3. Szuszczewicz, E.P., Holmes, J.C., Swinney, M., and Lin, C.S. (1981) DNA/PLACES barium event JAN: Quick-look field report on in-situ probe measurements, NRL Memorandum Report No. 4476.

severely depressed in the barium plasma. It can easily be shown that the increased molecular ion loss rate by electron recombination would deplete the molecular ions to less than 40 ions cm^{-3} in a matter of a few seconds in the vicinity of the barium peak concentration. On the other hand, the O^+ ions, which are atomic ions with an exceedingly small electron recombination rate, are essentially unaffected by the barium ion plasma except for some induced irregularity structure.

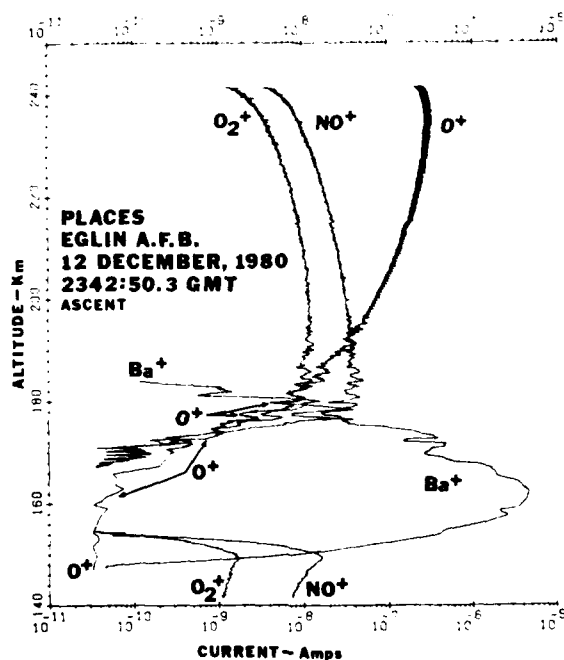


Figure 4. Ascent Measurements Showing the Penetration of the Barium Cloud and its Effects on the Normal Ambient Species NO^+ , O_2^+ , and O^+

If an unperturbed NO^+ profile is constructed in Figure 4 by extending the lower and upper altitude NO^+ profiles into the depletion, it is found that there is a definite enhancement in NO^+ of approximately 50% near 149 km, just below the barium cloud. The thickness of this enhanced layer is about 3 km. It is worth noting that this layer is not easily observed in the total ion density profile (see below aperture plate results) being smeared out by the sharply increasing barium ion density.

S. L. Ossakow, (Naval Research Laboratory, private communication, 1981) has suggested that the NO^+ bulge may represent the first experimental observation of an image cloud induced in the E region by electrostatic coupling with an F region barium cloud.^{4,5} Interestingly, irregularities or density fluctuations in O^+ , NO^+ , and O_2^+ persist well above the barium cloud to about 195 km; whereas the ionospheric structure above and (as shown later) throughout descent is strikingly smooth. Further, above about 176 km, the density fluctuations in NO^+ , O_2^+ , and O^+ are similar. Currently, there is no explanation for the wave-like structure that extends into the F region; indeed, Lloyd and Haerendel⁶ have noted that image cloud effects in the F region are negligible. Future modeling calculations are planned to determine the concentrations and extent of the E region image cloud. Also, attempts will be made to find the processes responsible for the higher altitude irregularities.

An expanded plot of the Ba^+ distribution also showing Ca^+ and Ba^{++} , is shown in Figure 5. The Ba^{++} ion was expected to be present because the second ionization potential of Ba^+ is only 9.95 eV and H Lyman α radiation is sufficiently energetic to produce the doubly ionized species. Since the barium payload was launched near 5° solar depression angle, H Lyman α illuminated the release for several minutes before being completely attenuated. The only significant chemical loss process known for Ba^{++} is $\text{Ba}^+ \cdot \text{NO} \rightarrow \text{NO}^+ + \text{Ba}^+$. This type of reaction has been measured for Ca^{++} and found to be very fast, but the analogous reaction with Ba^{++} has not been measured and must be very slow to explain the persistence of Ba^{++} about 20 min after the ionizing radiation is cut-off. Neither the photoionization cross section nor the atmospheric chemical loss processes for Ba^{++} are currently known.

From the manufacturer's analysis, the barium material utilized had a purity of 99.57% with a 0.04% each of Ca, Al, Mg, and Sr, as well as other impurities (Peter Kirschner, Thiokol Chemical Corp., private communication, 1981). No magnesium or aluminum ions were detected above the threshold limit of about 40 ions cm^{-3} . Unfortunately, no strontium ion measurements were programmed. The ratio of the number of calcium atoms to barium atoms in the atmospheric release was therefore about 1.4×10^{-3} . The Ca^+/Ba^+ ionic ratio varied from about 2.5×10^{-4} at low altitudes up to the barium peak and increased to about 10^{-3} at

4. Goldman, S. R., Ossakow, S. L., and Book, D. L. (1974) On the nonlinear motion of a small barium cloud in the ionosphere, J. Geophys. Res. 79:1471.
5. Scannapieco, A. J., Ossakow, S. L., Book, D. L., McDonald, B. E., and Goldman, S. R. (1974) Conductivity ratio effects on the drift and deformation of F region barium clouds coupled to the E region ionosphere, J. Geophys. Res. 79:2913.
6. Lloyd, K. H., and Haerendel, G. (1973) Numerical modeling of the drift and deformation of ionospheric plasma clouds and of their interaction with other layers of the ionosphere, J. Geophys. Res. 78:7389.

higher altitudes, with both ions reflecting similar structure. The increasing Ca^+/Ba^+ ratio with altitude does seem to be in agreement with the diffusion of barium and calcium ions according to their respective scale heights although this may be further complicated by the electromagnetic field- and wind-driven motions of these ions. While the barium ion cloud was optically observed to be moving in a northeasterly direction, the cloud center height was also seen to be falling at roughly 0.75 km min^{-1} (W. Boquist, Technology International Corp., private communication, 1981). No further attempt will be made here to examine quantitatively the motions or ionospheric processes of these ions; however, this effort may be worthwhile in the future to investigate possible mass dependent effects in the formation of ionospheric instabilities.

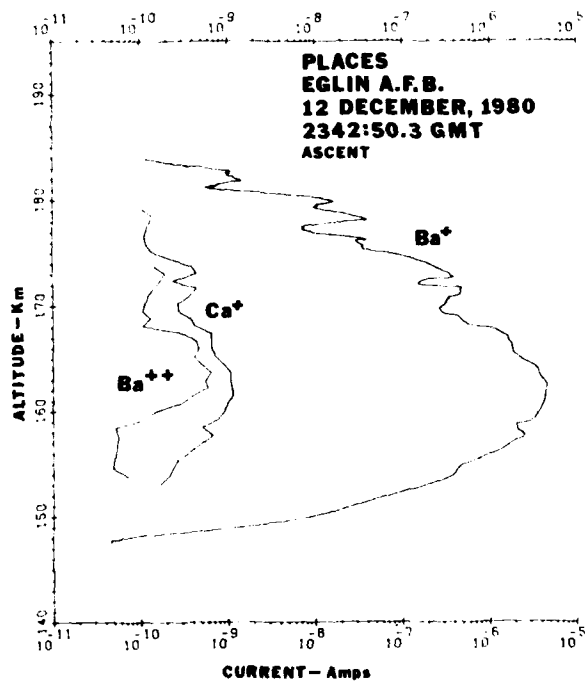


Figure 5. Distributions of Constituents From the Barium Release. Calcium is a typical impurity in barium

Plotted separately to reveal clearly the structure below 195 km are NO^+ (Figure 6), O_2^+ (Figure 7), and O^+ with H_2O^+ (Figure 8). The entire aperture plate current output is given in Figure 9, exhibiting measurements from 98 km to 241.2 km on ascent and to 80 km on descent. The plate current measurements are not as seriously affected by the large vehicle attack angles. Except for the depression near 178 km on descent caused by an ACS nitrogen jet fire, the ionospheric structure is exceedingly smooth outside the barium cloud. An expanded plot of the area of the barium cloud is shown in Figure 10. The aperture plate current and the pulsed probe profiles of Szuszczyewicz et al³ show a complete congruency in structure even to the tiniest density fluctuations.

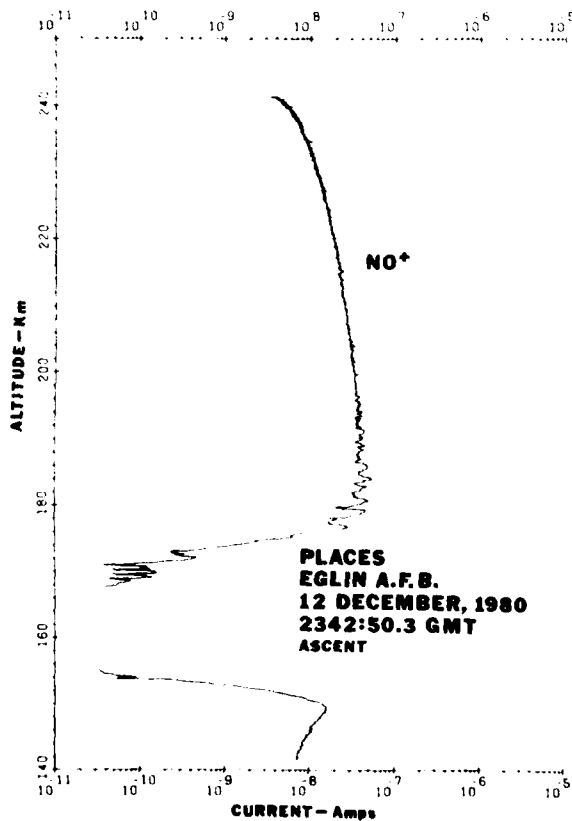


Figure 6. The NO^+ Profile Measured on Ascent

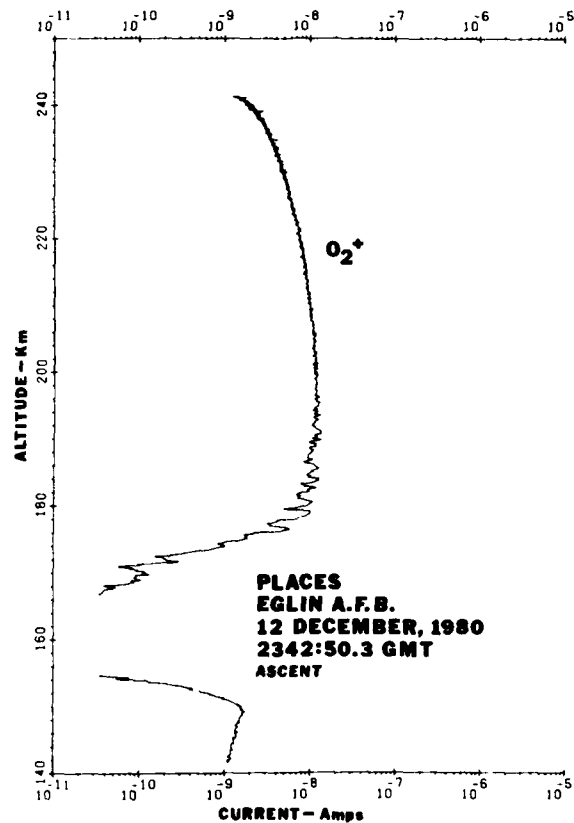


Figure 7. The O_2^+ Profile Measured on Ascent

Finally, we shall use the measured H_2O^+ concentrations to make a quantitative estimate of the outgassing water vapor concentrations near the payload surface. A quantitative measurement or determination of typical water vapor concentrations surrounding rocket vehicles has not been performed in the past and has long been needed to assess perturbations on a variety of rocket measurements. Rocket payloads are driven from atmospheric pressure to high vacuum in less than 2 min with total flight times of about 6 to 12 minutes. Since laboratory vacuum systems are known to outgas water vapor for long periods of time after initial pump-down, rocket surfaces will certainly have significant degassing rates over the entire flight. Further, experience has shown that the usual practice of purging payloads with dry nitrogen for several hours prior to launch does not drastically mitigate the degassing rates.

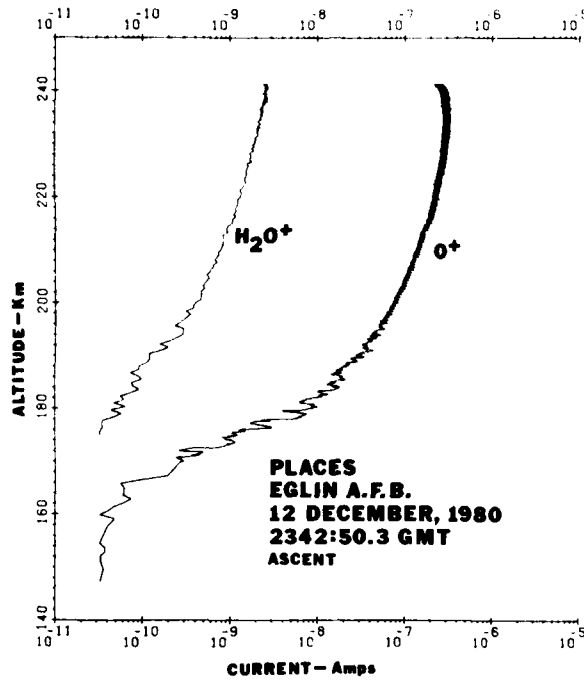


Figure 8. Ascent Measurements of O^+ and the Contaminant H_2O^+ . Note the structure similarity and the constant H_2O^+/O^+ ratio

To calculate the water vapor concentrations we utilize the fast charge transfer reaction, $O^+ + H_2O \rightarrow H_2O^+ + O$, $k = 2.3 \times 10^{-9} \text{ cm}^3 \text{ sec}^{-1}$, which produced the measured H_2O^+ ions. Referring to Figure 8, the H_2O^+/O^+ ratio is about 1% and is fairly constant with altitude, implying a relatively steady outgassing rate. The structural similarity between the O^+ and H_2O^+ distribution suggests that the H_2O^+ ions are produced near the vehicle. We now wish to determine exactly where the observed H_2O^+ ions are produced. We assume that the H_2O molecules leave the surface suffering no collisions until at least several meters from the payload and that back-scattering is generally small. This means that the H_2O molecules as well as the H_2O^+ ions are always moving away from the vehicle since there is typically no momentum transfer to the H_2O^+ ions in the reaction. Therefore, the measured H_2O^+ ions must be produced within the plasma sheath where the aperture plate potential can turn the ions around and draw them in. We further assume that the attractive potential is given by

$$V = 10e^{-\frac{x}{\lambda_d}} \text{ volts}$$

where x is the distance measured normal to the aperture plate and λ_d is the Debye length. The Debye lengths for 200 km and above vary from 0.5 cm to 0.8 cm over the plasma density range of $1.5 - 4 \times 10^5 \text{ cm}^{-3}$. The potential is sufficient to draw all the H_2O^+ ions into the spectrometer up to $x = 2.7$ cm and 4 cm, corresponding to the 0.5 cm and 0.8 cm Debye lengths, respectively. Note that these distances are essentially five Debye lengths so that the assumption of an exponentially decaying potential is not dramatically in error if it is accepted that by $10 \lambda_d$ the sheath edge is definitely attained. The time, Δt , available for the reaction to produce H_2O^+ ions is then the time it takes O^+ to traverse the distance x and is calculated from

$$x = u_0 \Delta t + 1/2 a (\Delta t)^2$$

where

$$a = eE/m, \text{ and}$$

$$E = -\frac{\partial V}{\partial x} = \frac{10}{\lambda_d} e^{-\frac{x}{\lambda_d}}$$

and u_0 is the speed of O^+ in the x direction. The O^+ speed is determined from the vehicle motion and its thermal speed, from which $u_0 \sim 10^5 \text{ cm sec}^{-1}$. Varying u_0 from 0 to $2 \times 10^5 \text{ cm sec}^{-1}$ changes Δt by less than a factor of two. Calculating Δt using the above values for x and λ_d , the average reaction time is found to be $17 \mu\text{sec}$ within 50%. The H_2O concentration can then be determined from

$$\Delta[\text{H}_2\text{O}^+]/\Delta t = k[\text{O}^+][\text{H}_2\text{O}],$$

since all H_2O^+ chemical loss processes are negligible in $17 \mu\text{sec}$. With $\Delta[\text{H}_2\text{O}^+]/[\text{O}^+] = 0.01$ and $\Delta t = 17 \mu\text{sec}$, $[\text{H}_2\text{O}] = 2.6 \times 10^{11} \text{ molecules cm}^{-3}$ to about a factor of two, which is the average concentration over the 4 cm distance from the surface. For $T = 300\text{K}$, (the surface temperature) this corresponds to a water vapor pressure of $8 \times 10^{-6} \text{ Torr}$, also to a factor of two uncertainty. This pressure range tends to support our collisionless assumption and is not atypical of observed laboratory outgassing pressures.

We plan in a future publication to examine past ionospheric rocket measurements to determine the spectrum of not only the H_2O concentrations near rocket surfaces but also as a function of distance from the surface.

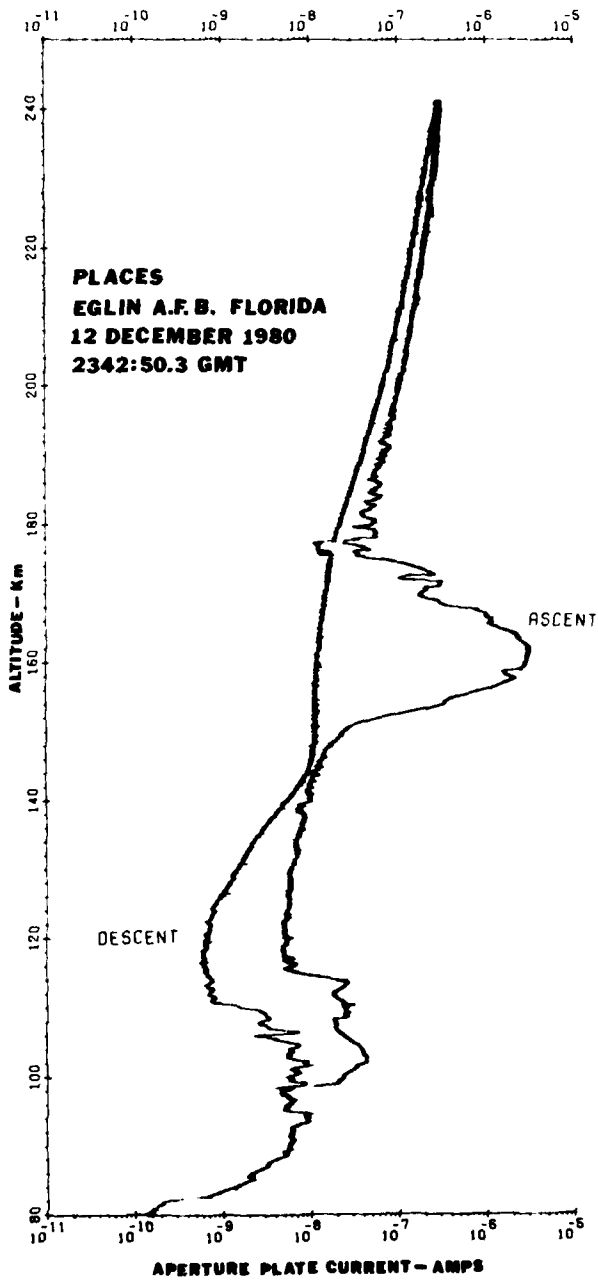


Figure 9. A Comparison of the Ascent and Descent Aperture Plate Current Measurements Showing the Smooth Ionosphere Adjacent to the Barium Cloud

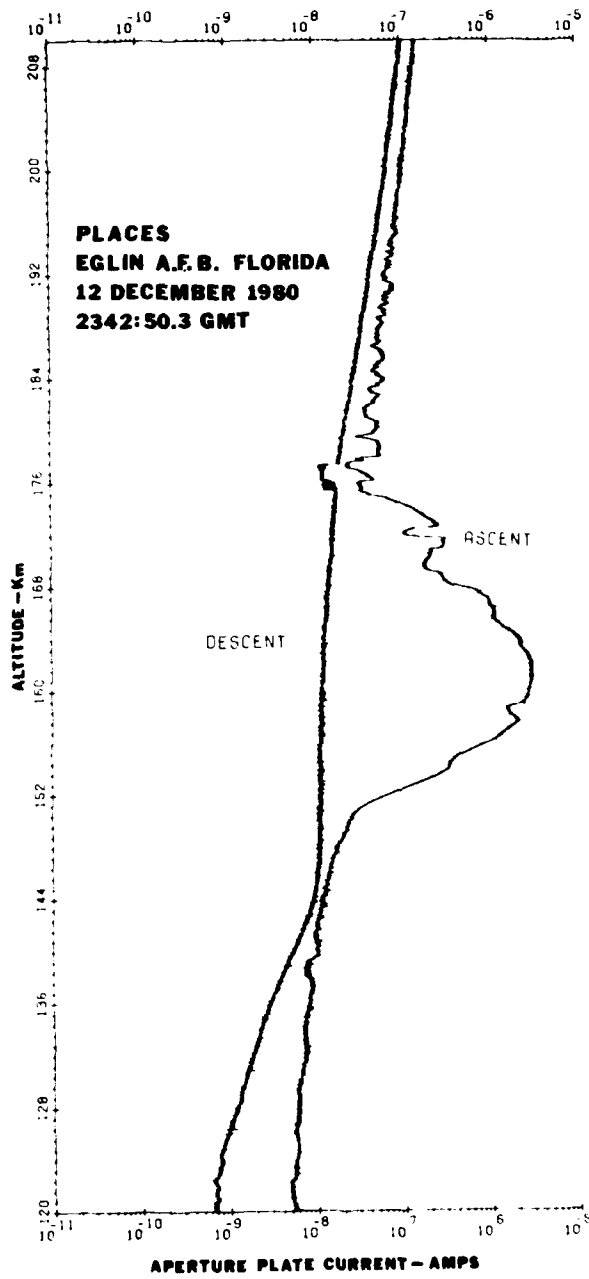


Figure 10. An Expanded Plot of the Ascent and Descent Aperture Plate Current Measurements in the Vicinity of the Barium Cloud

4. CONCLUSION

The first composition measurements in an ionospheric barium cloud have provided a wealth of information. Examination of the results led to the following observations:

(a) Several plasma chemical processes in the barium cloud were apparent from the ion species measurements, including the large recombinative loss of molecular ions, the Ba^+ chemistry, and the Ca^+ impurity ion chemistry.

(b) The microstructure of the plasma irregularities was accurately measured and further characterized by the species composition. Indeed the composition measurement provided the only way of determining that the density fluctuations above and below the barium cloud were not due to the barium ions.

(c) Mass dependent effects on the ion motions and instability development may be derived using the impurity tracer, Ca^+ (40 amu) and Ba^+ (138 amu) profiles.

(d) The first observation of an E region image cloud, which was visible only in the ion species distributions and not in the total density profile, have provided the initial measurements for a quantitative model assessment of these clouds.

(e) The wavelike structure in the natural ionospheric species extending into the F-region was unexpected and is currently not understood.

(f) A quantitative estimate of the outgassing water vapor concentrations near payload surfaces is provided for the first time utilizing the measured H_2O^+ ions. While outgassing contributed to only a 1% disturbance on the plasma measurements here, the perturbations on infrared and other rocket measurements may be more severe and these can now be assessed with increased accuracy.

References

1. Baker, K. D., and Ulwick, J. C. (1978) Measurements of electron density structure in striated barium clouds, Geophys. Res. Lett. 5:723.
2. Kelley, M. C., Baker, K. D., and Ulwick, J. C. (1979) Late time barium cloud striations and their possible relationship to equatorial Spread-F, J. Geophys. Res. 84:1898.
3. Szuszczewicz, E. P., Holmes, J. C., Swinney, M., and Lin, C. S. (1981) DNA/PLACES barium event JAN: Quick-look field report on in-situ probe measurements, NRL Memorandum Report No. 4476.
4. Goldman, S. R., Ossakow, S. L., and Book, D. L. (1974) On the nonlinear motion of a small barium cloud in the ionosphere, J. Geophys. Res. 79:1471.
5. Scannapieco, A. J., Ossakow, S. L., Book, D. L., McDonald, B. E., and Goldman, S. R. (1974) Conductivity ratio effects on the drift and deformation of F region barium clouds coupled to the E region ionosphere, J. Geophys. Res. 79:2913.
6. Lloyd, K. H., and Haerendel, G. (1973) Numerical modeling of the drift and deformation of ionospheric plasma clouds and of their interaction with other layers of the ionosphere, J. Geophys. Res. 78:7389.

DISTRIBUTION LIST

DEPARTMENT OF DEFENSE

Assistant Secretary of Defense
Comm, DMD, Cont. & Intell.
Washington, D. C. 20301
01CY ATTN J. Babcock
01CY ATTN M. Epstein

Director
Command Control Technical Center
Pentagon, Rm. BE 685
Washington, D. C. 20301
01CY ATTN C-650
01CY ATTN C-312, R. Mason

Director
Defense Advanced Rsch. Proj. Agency
Architect Building
1400 Wilson Blvd.
Arlington, VA. 22209
01CY ATTN Nuclear Monitoring
Research
01CY ATTN Strategic Tech. Office

Defense Communication Engineer Center
1860 Wiehle Avenue
Reston, VA. 22290
01CY ATTN Code R820
01CY ATTN Code R410,
James W. McLean
01CY ATTN R720, J. Worthington

Dept. of the Air Force
Headquarters Space Division
(AFSC) Los Angeles Air Force Station
P.O. Box 92960
Los Angeles, CA 90009
01CY Director, STP,
Col. D.E. Thursby
01CY Maj. C. Jund

Director
Defense Intelligence Agency
Washington, D. C. 20301
01CY ATTN DT-1B
01CY ATTN DB-4C, E. O'Farrell
01CY ATTN DIAAP, A. Wise
01CY ATTN DIAST-5
01CY ATTN DT-1BZ, R. Morton
01CY ATTN HQ #-TR, J. Stewart
01CY ATTN W. Wittig, DC-7D

Director
Defense Nuclear Agency
Washington, D. C. 20305
01CY ATTN STVL
04CY ATTN TITL
01CY ATTN DDST
03CY ATTN RAAE

Commander
Field Command
Defense Nuclear Agency
Kirtland AFB, NM 87115
01CY ATTN FCPR

Director
Interservice Nuclear Weapons School
Kirtland AFB, NM 87115
01CY ATTN FCPR

Director
Joint Strat. Tgt. Planning Staff
Offutt AFB,
Omaha, NB 68113
01CY ATTN JLTW-2
01CY ATTN JPST, G. Goetz

Joint Chiefs of Staff
Washington, D. C. 20301
01CY ATTN J-3 WWMCS
Evaluation Office

Chief
Livermore Division Fld. Command, DNA
Department of Defense
Lawrence Livermore Laboratory
P.O. Box 808
Livermore, CA 94550
01CY ATTN FCPRL

Director
National Security Agency
Department of Defense
Ft. George G. Meade, MD 20755
01CY ATTN John Skillman, R52
01CY ATTN Frank Leonard
01CY ATTN W14, Pat Clark
01CY ATTN Oliver H. Bartlett, W32
01CY ATTN R5

Commandant
NATO School (SHAPE)
APO New York 09172
01CY ATTN U. S. Documents Officer
Under Secy. of Def. for Rsch. & Engr.
Department of Defense
Washington, D. C. 20301
01CY ATTN Strategic & Space
Systems (OS)

Commander
U. S. Army Comm-Elec. Engrg. Instal. Agy.
Ft. Huachuca, AZ 85613
01CY ATTN CCC-EMEO, George Lane
WWMCCS System Engineering Org.
Washington, D. C. 20305
01CY ATTN R. Crawford

Commander/Director
Atmospheric Sciences Laboratory
U. S. Army Electronics Command
White Sands Missile Range, NM 88002
01CY ATTN DELAS-EO,
F. Niles

Director
BMD Advanced Tech. Ctr.
Huntsville Office
P.O. Box 1500
Huntsville, AL 35807
01CY ATTN ATC-T, Melvin T. Capps
01CY ATTN ATC-O, W. Davies
01CY ATTN ATC-R, Don Russ

Program Manager
BMD Program Office
5001 Eisenhower Avenue
Alexandria, VA 22333
01CY ATTN DACS-BMT, J. Shea

Chief C-E Service Division
U. S. Army Communications CMD
Pentagon, Rm. 1B269
Washington, D. C. 20310
01CY ATTN C-E-Services Division

Commander
FRADCOM Technical Support Activity
Department of the Army
Fort Monmouth, N. J. 07703
01CY ATTN DRSEL-NL-RD,
H. Bennet
01CY ATTN DRSEL-PL-ENV,
H. Bomke
01CY ATTN J. E. Quigely

Commander
Harry Diamond Laboratories
Department of the Army
2800 Powder Mill Road
Adelphi, MD 20783
(CNWDI-INNER ENVELOPE:
ATTN: DELHD-RBH)
01CY ATTN DELHD-TI, M. Weiner
01CY ATTN DELHD-RB, R. Williams
01CY ATTN DELHD-NP, F. Wimenitz
01CY ATTN DELHD-NP, C. Moazed

Commander
U. S. Army Comm-Elec. Engrg Instal.
Agy.
Ft. Huachuca, AZ 85613
01CY ATTN CCC-EMEO,
George Lane

Commander
U. S. Army Foreign Science & Tech. Ctr.
220 7th Street, NE
Charlottesville, VA 22901
01CY ATTN DRXST-SD
01CY ATTN R. Jones

Commander
U. S. Army Material Dev. & Readiness
CMD
5001 Eisenhower Avenue
Alexandria, VA 22333
01CY ATTN DRCLDC, J. A. Bender

Commander
U. S. Army Nuclear and Chemical Agency
7500 Backlick Road
Bldg. 2073
Springfield, VA 22150
01CY ATTN Library

Director
U. S. Army Ballistic Research Labs
Aberdeen Proving Ground, MD 21005
01CY ATTN Tech. Lib.,
Edward Baicy

Commander
U. S. Army SATCOM Agency
Ft. Monmouth, NJ 07703
01CY ATTN Document Control

Commander
U. S. Army Missile Intelligence Agency
Redstone Arsenal, AL 35809
01CY ATTN Jim Gamble

Director
U. S. Army TRADOC Systems Analysis
Activity
White Sands Missile Range, NM 88002
01CY ATTN ATAA-SA
01CY ATTN TCC/F. Payan, Jr.
01CY ATTN ATAA-TAC,
Ltc. J. Jesse

Commander
Naval Electronic Systems Command
Washington, D. C. 20360
01CY ATTN NAVLEN 034, T. Hughes
01CY ATTN PME 117
01CY ATTN PME 117-T
01CY ATTN Code 5011
01CY ATTN PME-106-T

Commanding Officer
Naval Intelligence Support Ctr.
4301 Suitland Road, Bldg. 5
Washington, D. C. 20390
01CY ATTN Mr. Dubbin, STIC 12
01CY ATTN NISC-50
01CY ATTN Code 5404, J. Galet

Commander
Naval Surface Weapons Center
Dahlgren Laboratory
Dahlgren, VA 22448
01CY ATTN Code DF-14, R. Butler

Office of Naval Research
Arlington, VA 22217
01CY ATTN Code 465
01CY ATTN Code 411
01CY ATTN Code 420
01CY ATTN Code 421

Commander
Aerospace Defense Command/DC
Department of the Air Force
Ent AFB, CO 80912
01CY ATTN DC, Mr. Long

Commander
Aerospace Defense Command/XPD
Department of the Air Force
Ent AFB, CO 80912
01CY ATTN XPDQQ
01CY ATTN XP

Air Force Geophysics Laboratory
Hanscom AFB, MA 01731
01CY ATTN OPR, Harold Gardner
01CY ATTN OPR-1,
James C. Ulwick
01CY ATTN LKB,
Kenneth S. W. Campion
01CY ATTN OPR, Alva T. Stair
01CY ATTN PHD, Jurgen Buchau
01CY ATTN PHD, John P. Mullen

AF Weapons Laboratory
Kirtland AFB, NM 87117
01CY ATTN SUL
01CY ATTN CA,
Auther H. Guenther
01CY ATTN NYTC, Capt. J. Barry
01CY ATTN NYTC, John M. Kamm
01CY ATTN NYTC,
Capt. Mark A. Fry
01CY ATTN NTES,
Maj. Gary Ganong
01CY ATTN NYTC, J. Janni

AFTAX
Patrick AFB, FL 32925
01CY ATTN TF/Maj. Wiley
01CY ATTN TN

Air Force Wright Aeronautical Labs
Wright-Patterson AFB, OH 45433
01CY ATTN AAAD, Wade Hunt
01CY ATTN AAAD, Allen Johnson

Deputy Chief of Staff
Research, Development, & ACQ
Department of the Air Force
Washington, D. C. 20330
01CY ATTN AFRDQ

Headquarters
Electronics Systems Division/XR
Department of the Air Force
Hanscom AFB, MA 01731
01CY ATTN XR, J. Deas

Headquarters
Electronic Systems Division/YSEA
Department of the Air Force
Hanscom AFB, MA 01731
01CY ATTN YSEA

Commander
Naval Ocean Systems Center
San Diego, CA 92152
03CY ATTN Code 532, W. Moler
01CY ATTN Code 0230, C. Baggett
01CY ATTN Code 81, R. Eastman
01CY ATTN Code 2200, H. Richter

Director
Naval Research Laboratory
Washington, D. C. 20375
01CY Code 4100
01CY Code 4101
01CY Code 4120
01CY Code 4701, Jack D. Brown
20CY Code 2628
01CY Code 4732, E. McLean
01CY Code 6000
01CY Code 7000
01CY Code 7500
01CY Code 7580
01CY Code 7551
01CY Code 7555
01CY Code 7900

Commander
Naval Sea Systems Command
Washington, D. C. 20362
01CY ATTN Capt. R. Pitkin

Commander
Naval Space Surveillance System
Dahlgren, VA 22448
01CY ATTN Capt. J.H. Burton

Officer-in-Charge
NAL Surface Weapons Center
White Oak, Silver Spring, MD 20910
01CY ATTN Code F31

Director, Strategic Systems Project
Office
Department of the Navy
Washington, D. C. 20376
01CY ATTN NSP-2141
01CY ATTN Nssp-2722,
Fred Wimberly

Naval Space System Activity
P.O. Box 92960
Worldway Postal Center
Los Angeles, CA 90009
01CY ATTN LCDR, Donald Snoddy
01CY ATTN Commanding Officer

Headquarters
Electronics Systems Division/DC
Department of the Air Force
Hanscom AFB, MA 01731
01CY ATTN DCKC, Maj. J. C. Clark

Commander
Foreign Technology Division, AFSC
Wright-Patterson AFB, OH 45433
01CY ATTN NICD, Library
01CY ATTN ETDP, B. Ballard

Commander
Rome Air Development Center, AFSC
Griffiss AFB, NY 13441
01CY ATTN DOC Library/TSLD
01CY ATTN OCSE, V. Coyne

SAMSO/SZ
Post Office Box 92960
Worldway Postal Center
Los Angeles, CA 90009
(SPACE DEFENSE SYSTEMS)
01CY ATTN SZJ

Strategic Air Command/XPFS
Offutt AFB, NB 68113
01CY ATTN XPFS, Maj. B. Stephan
01CY ATTN ADWATE,
Maj. Bruce Bauer
01CY ATTN NRT
01CY ATTN DOK, Chief Scientist

SAMSO/YA
P.O. Box 92960
Worldway Postal Center
Los Angeles, CA 90009
01CY ATTN YAT,
Capt. L. Blackwelder

SAMSO/SK
P.O. Box 92960
Worldway Postal Center
Los Angeles, CA 90009
01CY ATTN SKA (Space Como Systems)
M. Clavin

SAMSO/MN
Norton AFB, CA 92409
(MINUTEMAN)
01CY ATTN MNNL, L. T. C. Kennedy

Commander
Rome Air Development Center, AFSC
Hanscom AFB, MA 01731
01CY ATTN EEP, A. Lorentzen

DEPARTMENT OF ENERGY

Department of Energy
Albuquerque Operations Office
P.O. Box 5400
Albuquerque, NM 87115
01CY ATTN Doc Con for
D. Sherwood

Department of Energy
Library Room G-042
Washington, D.C. 20545
01CY ATTN Doc Con for
A. Labowitz

EG&G, Inc.
Los Alamos Division
P.O. Box 809
Los Alamos, NM 85544
01CY ATTN Doc Con for
J. Breedlove

University of California
Lawrence Livermore Laboratory
P.O. Box 808
Livermore, CA 94550
01CY ATTN Doc con for
Tech. Info. Dept.
01CY ATTN Doc Con for L-389,
R. Ott
01CY ATTN Doc Con for L-31,
R. Hager
01CY ATTN Doc Con for L-46,
F. Seward

Los Alamos Scientific Laboratory
P.O. Box 1663
Los Alamos, NM 87545
01CY ATTN Doc Con for
J. Wolcott
01CY ATTN Doc Con for
R. F. Taschek
01CY ATTN Doc Con for
E. Jones
01CY ATTN Doc Con for J. Malik
01CY ATTN Doc Con for
R. Jeffries
01CY ATTN Doc Con for J. Zinn
01CY ATTN Doc Con for P. Keaton
01CY ATTN Doc Con for
D. Westervelt
01CY ATTN Doc Con for
M. Pongratz

Sandia Laboratories

P.O. Box 5800

Albuquerque, NM 87115

01CY ATTN Doc Con for J. Martin

01CY ATTN Doc Con for W. Brown

01CY ATTN Doc Con for

A. Thornbrough

01CY ATTN Doc Con for T. Wright

01CY ATTN Doc Con for D. Dahlgren

01CY ATTN Doc Con for 3141

01CY ATTN Doc Con for Space

Project Div.

Sandia Laboratories

Livermore Laboratory

P.O. Box 969

Livermore, CA 94550

01CY ATTN Doc Con for B. Murphy

01CY ATTN Doc Con for T. Cook

Office of Military Application

Department of Energy

Washington, D.C. 20545

01CY ATTN Doc Con for D. Gale

OTHER GOVERNMENT

Central Intelligence Agency

ATTN RD/SL, Rm. 5G48, Hq. Bldg.

Washington, D.C. 20505

01CY ATTN OSI/PSID, Rm. 5F 19

Department of Commerce

National Bureau of Standards

Washington, D.C. 20234

(ALL CORRES: ATTN SEC

OFFICER FOR)

01CY ATTN R. Moore

Department of Transportation

Office of the Secretary

TAD-44.1, Room 10402-B

400 7th Street, S.W.

Washington, D.C. 20590

01CY ATTN R. Lewis

01CY ATTN R. Doherty

Institute for Telecom Sciences

National Telecommunications & Info.

Admin.

Boulder, CO 80303

01CY ATTN A. Jean (Unclass. only)

01CY ATTN W. Utlaut

01CY ATTN D. Crombie

01CY ATTN L. Berry

National Oceanic & Atmospheric Admin.

Environmental Research Laboratories

Department of Commerce

Boulder, CO 80302

01CY ATTN R. Grubb

01CY ATTN Aeronomy Lab, G. Reid

DEPARTMENT OF DEFENSE

CONTRACTORS

Aerospace Corporation

P.O. Box 92957

Los Angeles, CA 90009

01CY ATTN I. Garfunkel

01CY ATTN T. Salmi

01CY ATTN V. Josephson

01CY ATTN S. Bower

01CY ATTN N. Stockwell

01CY ATTN D. Olsen

01CY ATTN J. Carter

01CY ATTN F. Morse

01CY ATTN SMFA for PWW

01CY ATTN J. Fennel

01CY ATTN C. Rice

01CY ATTN H. Koons

Analytical Systems Engineering Corp.

5 Old Concord Road

Burlington, MA 01803

01CY ATTN Radio Sciences

Berkeley Research Associates, Inc.

P.O. Box 983

Berkeley, CA 94701

01CY ATTN J. Workman

Boeing Company, The

P.O. Box 3707

Seattle, WA 98124

01CY ATTN G. Keister

01CY ATTN D. Murray

01CY ATTN G. Hall

01CY ATTN J. Kenney

California at San Diego, Univ. of

IPAPS, B-019

La Jolla, CA 92093

01CY ATTN Henry G. Booker

01CY ATTN E.C. Whipple

Brown Engineering Company, Inc.

Cummings Research Park

Huntsville, AL 35807

01CY ATTN Romeo A. Deliberis

Charles Stark Draper Laboratory, Inc.

555 Technology Square

Cambridge, MA 02139

01CY ATTN D.B. Cox

01CY ATTN J.P. Gilmore

Computer Sciences Corporation

6565 Arlington Blvd

Falls Church, VA 22046

01CY ATTN H. Blank

01CY ATTN John Spoor

01CY ATTN C. Nail

Comstat Laboratories
Linthicum Road
Clarksburg, MD 20734
01CY ATTN G. Hyde

Electrospace Systems, Inc.
Box 1359
Richardson, TX 75080
01CY ATTN H. Logston
01CY ATTN Security (Paul Phillips)

ESL INCL.
495 Java Drive
Sunnyvale, CA 94086
01CY ATTN J. Roberts
01CY ATTN James Marshall
01CY ATTN C. W. Prettie

Ford Aerospace and Communications
Corp.
3939 Fabian Way
Palo Alto, CA 94303
01CY ATTN J. T. Mattingley

General Electric Company
Space Division
Valley Forge Space Center
Goddard Blvd., King of Prussia
P. O. Box 8555
Philadelphia, PA 19101
01CY ATTN M. H. Bortner
Space Sci. Lab.

General Electric Company
P. O. Box 1122
Syracuse, NY 13201
01CY ATTN F. Reibert

General Electric Company
Tempo-Center for Advanced Studies
816 State Street (P. O. Drawer QQ)
Santa Barbara, CA 93102
01CY ATTN DASIAC
01CY ATTN Don Chandler
01CY ATTN Tom Barrett
01CY ATTN Tim Stephans
01CY ATTN Warren S. Knapp
01CY ATTN William McNamara
01CY ATTN B. Gambill
01CY ATTN Mack Stanton

General Electric Tech. Services Co.,
Inc.
HMES
COURT
Syracuse, NY 13201
01CY ATTN G. Millman

General Research Corporation
Santa Barbara Division
P. O. Box 6770
Santa Barbara, CA 93111
01CY ATTN Joe Ise, Jr.
01CY ATTN Joel Garbarino

Geophysical Institute
University of Alaska
Fairbanks, AK 99701
(ALL CLASS ATTN: SECURITY OFFICERS)
01CY ATTN T. N. Davis (Uncl. Only)
01CY ATTN Neal Brown (Uncl. Only)
01CY ATTN Technical Library
01CY ATTN T. Hallinan

Illinois, University of
ATTN: Dan McClellan for K. C. Yeh
150 Davenport House
Champaign, IL 61820

Institute for Defense Analyses
400 Army-Navy Drive
Arlington, VA 22202
01CY ATTN J. M. Aein
01CY ATTN Hans Wolfhard
01CY ATTN Joel Bengston

HSS, Inc.
2 Alfred Circle
Bedford, MA 01730
01CY ATTN Donald Hansen

Intl. Tel. & Telegraph Corporation
500 Washington Avenue
Nutley, NJ 07110
01CY ATTN Technical Library

JAYCOR
1401 Camino Del Mar
Del Mar, CA 92014
01CY ATTN S. R. Goldman

Johns Hopkins University
Applied Physics Laboratory
Johns Hopkins Road
Laurel, MD 20810
01CY ATTN Document Librarian
01CY ATTN Thomas Potemra
01CY ATTN John Dassoulas

Lockheed Missiles & Space Co., Inc.
P. O. Box 504
Sunnyvale, CA 94088
01CY ATTN Dept. 60-12
01CY ATTN D. R. Churchill

Lockheed Missiles and Space Co., Inc.
3251 Hanover Street
Palo Alto, CA 94304
01CY ATTN Martin Walt, Dept. 52-10
01CY ATTN Richard G. Johnson
Dept. 52-12
01CY ATTN W. L. Imhof, Dept. 52-12
01CY ATTN D. Cauffman

Kaman Sciences Corp.
P.O. Box 7463
Colorado Springs, CO 80933
01CY ATTN T. Meagher

Linkabit Corp.
10453 Roselle
San Diego, CA 92121
01CY ATTN Irwin Jacobs
01CY ATTN I. Rothmueller

Lowell Rsch. Foundation, University of
450 Aiken Street
Lowell, MA 01854
01CY ATTN K. Bibl
01CY ATTN B. Reinisch

M. I. T. Lincoln Laboratory
P.O. Box 73
Lexington, MA 02173
01CY ATTN David M. Towle
01CY ATTN P. Waldron
01CY ATTN L. Loughlin
01CY ATTN D. Clark
01CY ATTN J. Davis

Martin Marietta Corp.
Orlando Division
P.O. Box 5837
Orlando, FL 32805
01CY ATTN R. Heffner

McDonnell Douglas Corporation
5301 Bolsa Avenue
Huntington Beach, CA 92647
01CY ATTN N. Harris
01CY ATTN J. Moule
01CY ATTN George Mroz
01CY ATTN W. Olson
01CY ATTN R. W. Halprin
01CY ATTN Technical Library
Services

Mission Research Corporation
735 State Street
Santa Barbara, CA 93101
01CY ATTN P. Fischer
01CY ATTN W.F. Crevier
01CY ATTN Steven L. Gutsche
01CY ATTN D. Sappenfield
01CY ATTN R. Bogusch
01CY ATTN Ralph Kilb
01CY ATTN R. Hendrick
01CY ATTN Dave Sowle
01CY ATTN F. Fajen
01CY ATTN M. Scheibe
01CY ATTN Conrad L. Longmire
01CY ATTN Warren A. Schlueter

Mitre Corporation, The
P.O. Box 208
Bedford, MA 01730
01CY ATTN John Morganstern
01CY ATTN G. Harding
01CY ATTN C.E. Callahan

Mitre Corp.
Westgate Research Park
1820 Dolly Madison Blvd.
McLean, VA 22101
01CY ATTN W. Hall
01CY ATTN W. Foster

Pacific-Sierra Research Corp.
1456 Cloverfield Blvd.
Santa Monica, CA 90404
01CY ATTN E.C. Field, Jr.

Pennsylvania State University
Ionosphere Research Lab
318 Electrical Engineering East
University Park, PA 16802
(NO CLASSIFIED TO THIS ADDRESS)
01CY ATTN Ionospheric Research Lab

Photometrics, Inc.
442 Marrett Road
Lexington, MA 02173
01CY ATTN Irving L. Kofsky

Physical Dynamics Inc.
P.O. Box 3027
Bellevue, WA 98009
01CY ATTN E.J. Fremouw

Physical Dynamics Inc.
P.O. Box 1069
Berkeley, CA 94701
01CY ATTN A. Thompson

R & D Associates
P.O. Box 9695
Marina Del Rey, CA 90291
01CY ATTN Forrest Gilmore
01CY ATTN Bryan Gabbard
01CY ATTN William B. Wright, Jr.
01CY ATTN William J. Karzas
01CY ATTN Robert F. Lelevier
01CY ATTN H. Ory
01CY ATTN C. Macdonald
01CY ATTN R. Turco

Rand Corporation, The
1700 Main Street
Santa Monica, CA 90406
01CY ATTN Cullen Crain
01CY ATTN Ed Bedrozian

Riverside Research Institute
80 West End Avenue
New York, NY 10023
01CY ATTN Vince Trapani

Science Application, Inc.
P.O. Box 2351
La Jolla, CA 92038

01CY ATTN Lewis M. Linson
01CY ATTN Daniel A. Hamlin
01CY ATTN D. Sachs
01CY ATTN E.A. Straker
01CY ATTN Curtus A. Smith
01CY ATTN Jack McDougall

Raytheon Co.
528 Boston Post Road
Sudbury, MA 01776
01CY ATTN Barbara Adams

Science Applications, Inc.
Huntsville Division
2109 W. Clinton Avenue
Suite 700
Huntsville, AL 35805
01CY ATTN Dale H. Davis
Science Applications, Incorporated
8400 Westpark Drive
McLean VA 22101
01CY ATTN J. Cockayne

Science Applications, Inc.
80 Mission Drive
Pleasanton, CA 94566
01CY ATTN SZ

SRI International
333 Ravenswood Avenue
Menlo Park, CA 94025
01CY ATTN Donard Neilson
01CY ATTN Alan Burns
01CY ATTN G. Smith
01CY ATTN L.L. Cobb
01CY ATTN David A. Johnson
01CY ATTN Walter G. Chesnut
01CY ATTN Charles L. Rino
01CY ATTN Walter Jaye
01CY ATTN M. Baron
01CY ATTN R. Livingston
01CY ATTN Ray L. Leadabrand
01CY ATTN G. Carpenter
01CY ATTN G. Price
01CY ATTN J. Peterson
01CY ATTN R. Hake, Jr.
01CY ATTN V. Gonzales
01CY ATTN D. McDaniel
01CY ATTN R. Tsunoda

Technology International Corp.
75 Wiggins Avenue
Bedford, MA 01730
01CY ATTN W.P. Boquist

University of Tokyo
ISAS
Komaba, Meguro-Ku
Tokyo, Japan
01CY ATTN Dr. K.I. Oyama

Max-Planck-Institut
Für Physik Und Astrophysik
Institut für Extraterrestrische Physik
8046 Garching B. München, Germany
01CY ATTN Prof. Gerhard Haerendel

TRW Defense & Space Sys. Group
One Space Park
Redondo Beach, CA 90278
01CY ATTN R.K. Plebuch
01CY ATTN S. Altschuler
01CY ATTN D. Dee

Visidyne, Inc.
19 Third Avenue
North West Industrial Park
Burlington, MA 01802
01CY ATTN Charles Humphrey
01CY ATTN J.W. Carpenter

DA
FIL
04